

# A Comparative Study on Photocatalytic Performance of Perovskite Materials Synthesized from Discarded Rare Earth Magnet with the one from Pure Neodymium Salt

Huy Pham Khanh, Huyen Nguyen Thi Thu, Thuy Hoang Thi Bich\*, Tung Mai Thanh, Hai Huynh Trung

Hanoi University of Science and Technology, 1 Dai Co Viet Road, Ha Noi, Vietnam  
 thuy.hoangthibich1@hust.edu.vn

Perovskite-type rare earth orthoferrite ( $\text{ReFeO}_3$ ) nanocrystalline were synthesized by using sol-gel citrate method and followed by calcination from oxalate salt  $\text{Re}_2(\text{C}_2\text{O}_4)_3$ , which composed of Nd (76.5 %), Pr (14.8 %), Dy (5.5 %) and Tb (3.2 %) recovered from discarded neodymium magnets (NdFeB) in hard-disk-drive waste. The synthesized materials were characterized by X-ray diffraction (XRD), field emission scanning electron microscopes (SEM), Brunauer–Emmett–Teller nitrogen adsorption and desorption (BET), Ultraviolet-visible diffuse reflection spectroscopy (UV–Vis DRS). The perovskite  $\text{NdFeO}_3$  was synthesized under the same conditions from an analytical grade pure salt to be used as a control material. Photocatalytic characteristics of both perovskite  $\text{ReFeO}_3$  and  $\text{NdFeO}_3$  were investigated through evaluation of methylene blue (MB) degradation under visible light. The degradation efficiency of MB by the  $\text{ReFeO}_3$  catalyst was higher than that by  $\text{NdFeO}_3$  after 3 h of illumination under visible light. The degradation efficiency could reach 99.2 % and the photocatalytic capacity remained after 5 cycles for  $\text{ReFeO}_3$  catalyst.

## 1. Introduction

Nowadays, electronic waste (e-waste) is well known as a cause of serious pollution to our planet. The global e-waste monitor estimated that amount of e-waste over the world will reach 49.8 Bt in 2020 (Baldé et al., 2015). In Vietnam, this amount will be 567,000 tons in 2025 based on forecasting data of the United Nations Industrial Development Organization - UNIDO (Nguyen et al., 2009). Finding proper treatment method for this kind of waste is necessary to avoid the extreme outcomes, e.g. negative impacts on the human health and living environment. On the other hand, fast development and over manufacture in many industrial sectors lead to exhaustion of resources, one of which is rare earth element (Charalampides et al., 2015). In this context, the treatment, recovery and recycling precious metals in e-waste are in urgent demand to avoid environmental issues and to use mineral resources effectively.

Since  $\text{ABO}_3$  perovskite materials show plenty of interesting properties such as metal-insulator transition, high curie temperature superconductivity, and colossal magnetoresistance, they have been used for various applications, e.g. fuel-cell electrode materials (Gao et al., 2016), gas sensor (Willa et al., 2017), photocatalysts (Luu et al., 2016) or solar cell materials. Recently, photocatalysts originated from rare earth have been concerned for environmental treatment (Tahir, 2018) or create gas products (Vaiano et al., 2017). So far, most rare earth photocatalysts have been synthesized from pure rare earth salts. Few literatures reported on synthesis of photocatalysts from e-waste sources. Research results show that this is a material with high photocatalytic ability. To clarify the above suspicion, in this work, rare earth elements recovered from permanent magnet NdFeB of hard disk drive waste with the main composition of neodymium in the form of  $\text{Re}_2(\text{C}_2\text{O}_4)_3$  were used to synthesize perovskite material  $\text{ReFeO}_3$ . The methylene blue degradation in aqueous media in the presence of the synthesized  $\text{ReFeO}_3$  materials under visible light was investigated in detail.

## 2. Experimental

### 2.1 Materials

Permanent magnets NdFeB were collected from discarded hard disks in Vietnam. All other chemicals such as  $\text{Nd}(\text{NO}_3)_3 \cdot 6\text{H}_2\text{O}$ ,  $\text{Fe}(\text{NO}_3)_3 \cdot 9\text{H}_2\text{O}$ , citric acid, oxalic acid, sulfuric acid, nitric acid, ammonia and methylene blue were purchased from Sigma-Aldrich.

### 2.2 Synthesis of perovskite materials

The rare earth oxalate  $\text{Re}_2(\text{C}_2\text{O}_4)_3$  was recovered from permanent magnets and used as starting material for synthesis of perovskite  $\text{ReFeO}_3$  material (Pham et al., 2017). In particular,  $\text{ReFeO}_3$  was synthesized via sol-gel citrate method according to the previously reported process (Hao et al., 2011). For comparison,  $\text{NdFeO}_3$  was also prepared as a control material. In this synthesis procedure, a mixture solution with molar ratio of 1:1:3 for Re:Fe:citric acid was continuously stirred with a magnetic stirrer at 80 °C for 5 h using a reflux device. Next, obtained solution was continuously stirred at 80 °C to remove excess water and to form a viscous transparent lemon-yellow gel, which was followed by a drying process at 80 °C for 12 h to form a dry gel. After that, gel was heated at 350 °C for 1 h and maintained at 700 °C for 5 h before quenching to room temperature to form perovskite-type crystals.

### 2.3 Characterization

The crystalline phase structure of synthesized materials was measured on a Bruker D8-Advance with X-ray diffractometer (XRD) using  $\text{CuK}\alpha$  radiation. The Brunauer–Emmett–Teller (BET) surface area was measured on Micromeritics Gemini VII 2390t by the  $\text{N}_2$  adsorption. The morphology of the materials was observed by SEM on a Hitachi S-4800 JED. Energy dispersive X-ray spectroscopy analysis (EDX) was done on an EMAX 7593-H, Horiba. UV-Vis diffuse reflection spectroscopy (DRS) was performed on a Shimadzu UV2550 spectrophotometer.

Optical band gap is determined using Tauc's plot as shown in Eq(1).

$$\alpha h\nu = (A h\nu - E_g)^{n/2} \quad (1)$$

Wherein, A is a constant, h is the Plank constant,  $\nu$  is the light frequency,  $E_g$  is the optical energy band gap value, exponent n depends on the type of transition and  $\alpha$  is the absorption coefficient.

### 2.4 Photocatalytic activity test

Photocatalytic activity of synthesized materials including  $\text{ReFeO}_3$  and  $\text{NdFeO}_3$ , was determined by degradation of methylene blue. Tests were performed in a cylindrical vessel reactor surrounded by water jacket to keep reaction at room temperature. Depending on testing purpose, an exact amount of perovskite materials and MB solution were added into the reactor. In the experiment, a 125 W high pressure mercury lamp with photo intensity of  $60.13 \text{ w/m}^2$ , which was measured by Broadband Power/Energy Meter 13PEM001, was used as a visible light source for the degradation test. Before illumination, the solution containing MB and the photocatalyst was stirred in the dark for 90 min to reach the adsorption–desorption equilibrium. After that, the solution would be added by a suitable amount of  $\text{H}_2\text{O}_2$  and illuminated under visible light. In an interval of 30 min, a sample was taken from the reactor to remove the photocatalyst by using a centrifuge. The concentration of MB in the remained solution was measured by UV-Vis spectrophotometer at a wavelength  $\lambda_{\text{max}} = 664 \text{ nm}$ . The degradation efficiency (or conversion efficiency) of MB ( $\eta$ ) was then calculated from the initial concentration of MB ( $C_0$ ) and concentration ( $C_t$ ) at the reaction time (t) as in following Eq(2).

$$\eta = ((C_0 - C_t)/C_0) \times 100 \quad (2)$$

## 3. Results and discussions

### 3.1 XRD, morphological and BET analysis

The XRD patterns of the synthesized  $\text{ReFeO}_3$  and  $\text{NdFeO}_3$  are presented in Figure 1a. It can be seen that the synthesized materials show orthorhombic structure of the perovskite type (JCPDS card No. 153441). XRD pattern of  $\text{ReFeO}_3$  has a little bit different from the material  $\text{NdFeO}_3$  synthesized from pure salt. That is attributed to the presence of several rare earth elements apart from neodymium element in the perovskite  $\text{ReFeO}_3$ . From Figure 1b and 1c, it is recognized that both  $\text{ReFeO}_3$  and  $\text{NdFeO}_3$  composed of interconnected nanoparticles with grain size ranging from 50 to 100 nm.

Table 1 lists the physicochemical parameters obtained from  $\text{N}_2$  adsorption-desorption isotherm measurements of  $\text{ReFeO}_3$  and  $\text{NdFeO}_3$ . The analysis results showed that the pore volume and pore size of  $\text{ReFeO}_3$  were  $0.413543 \text{ cm}^3/\text{g}$  and  $104.11 \text{ nm}$ , respectively. These values were higher than those of  $\text{NdFeO}_3$ . In contrast,

$\text{NdFeO}_3$  revealed a high specific surface area compared with  $\text{ReFeO}_3$ . These parameters might be the advantageous properties for the degradation of MB to take place (Yahya et al., 2018).

Table 1: Textural properties of  $\text{ReFeO}_3$  and  $\text{NdFeO}_3$  samples.

Compound	Surface area ( $\text{m}^2/\text{g}$ )	Pore volume ( $\text{cm}^3/\text{g}$ )	Pore size (nm)
$\text{ReFeO}_3$	10.1963	0.413543	104.11
$\text{NdFeO}_3$	11.5730	0.208117	48.65

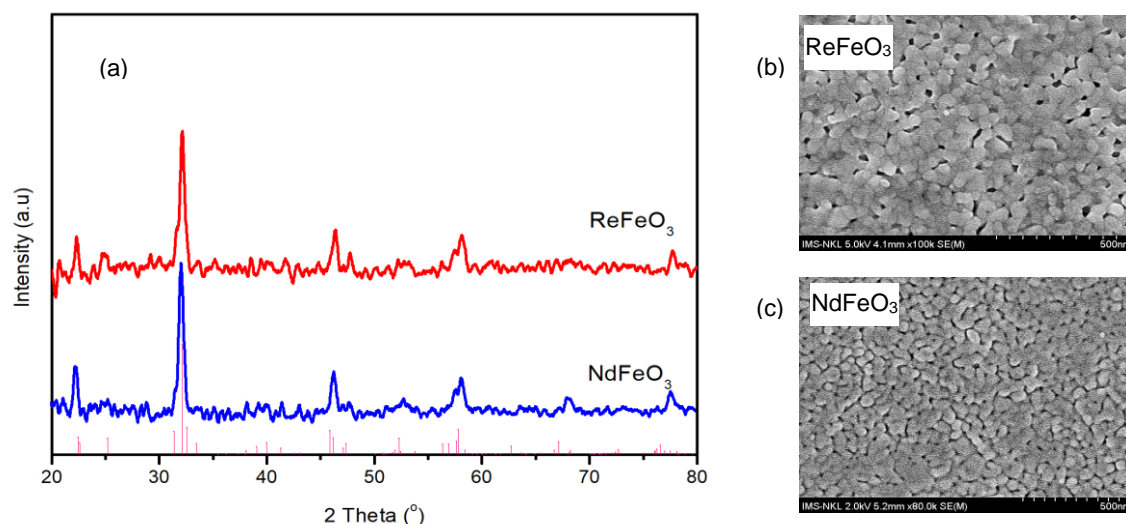


Figure 1: (a) XRD patterns of synthesized  $\text{ReFeO}_3$ ,  $\text{NdFeO}_3$  and  $\text{NdFeO}_3$  reference (JCPDS card No. 153441) and (b) SEM images of  $\text{ReFeO}_3$  and (c) SEM images of  $\text{NdFeO}_3$ .

### 3.2 Band gap characterization

The UV-Vis DRS of synthesized materials was recorded by the Shimadzu UV2550 spectrophotometer and shown in Figure 2a. Accordingly, the band gap energy of  $\text{ReFeO}_3$  and  $\text{NdFeO}_3$  was estimated to be 1.81 eV and 1.80 eV, respectively, as shown in Figure 2b and 2c. These values reveal that synthesized materials have suitable capability of visible-region light absorption and thus, degrading organic compounds under visible light irradiation (Sacco et al., 2015).

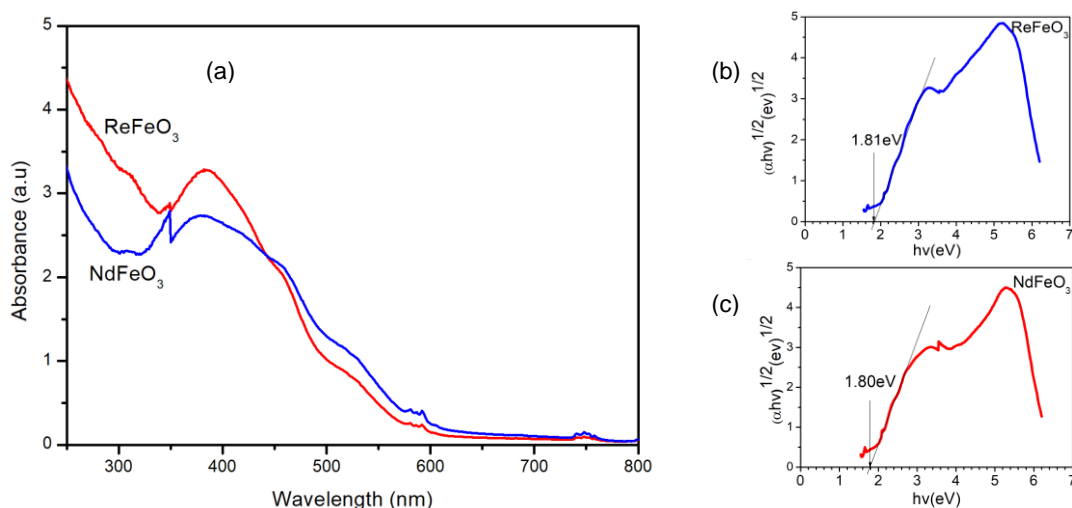


Figure 2: (a) UV-Vis diffuse reflectance spectra; Band-gap energies ( $E_g$ ) of (b) synthesized  $\text{ReFeO}_3$  and (c)  $\text{NdFeO}_3$ .

### 3.3 Photocatalytic activity of synthesized materials

Figure 3a illustrates the photocatalysis of ReFeO<sub>3</sub> for the degradation of MB under visible light irradiation. The measured results indicate that the concentration of remained MB decreased with the increase in catalyst dose. However, further increase in the catalyst dose over 0.4 mg/L resulted in a slight increase in the concentration of the remained MB. The degradation efficiency of MB at dose of 0.5 mg/L was lower than that at the dose of 0.4 mg/L. This is attributed to the presence of abundant catalysts in the test solution. This prevented penetration of incident light rays through the solution (Phan et al., 2017).

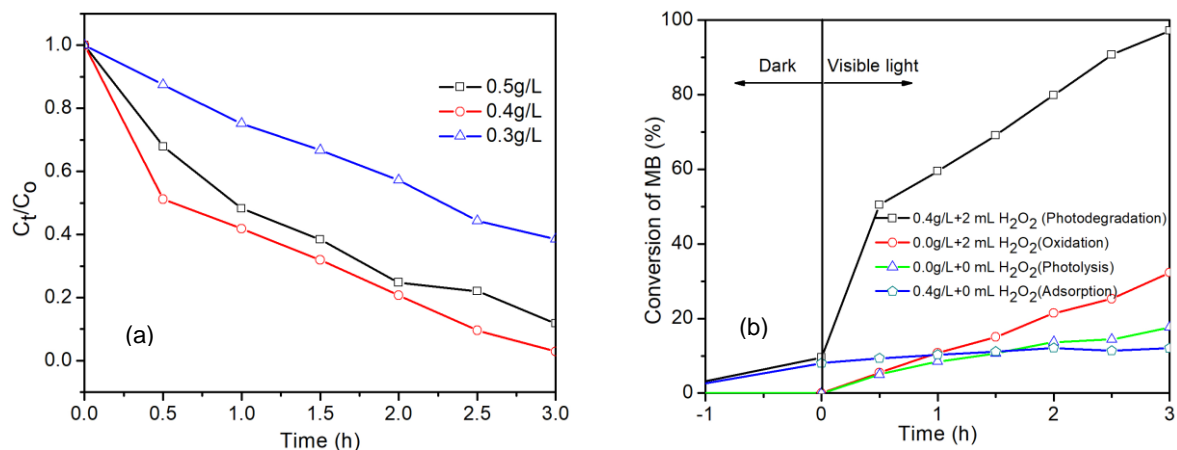
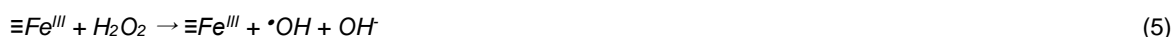


Figure 3: (a) Effect of ReFeO<sub>3</sub> catalyst dose on the photodegradation of MB (Conditions:  $V_{MB} = 100$  mL;  $t = 35$  °C;  $H_2O_2$  30% = 2 mL) and (b) Conversion of MB via adsorption, photolysis, oxidation by  $H_2O_2$  and photodegradation (temperature = 35 °C; MB = 5 mg/L;  $m_{ReFeO_3} = 0.4$  g/L).

From measurements and calculations, it can be seen that the conversion efficiency of MB by adsorption process was 12.0 %, by photolysis process was 19.2 %, by oxidation process was 39.3 % and by photodegradation process was 99.2 % (Figure 3b). Based on above results and previous reports, the conversion of MB in the presence of the ReFeO<sub>3</sub> catalyst can be explained by three main mechanisms as follows: (i) heterogeneous Fenton-like catalytic mechanism; (ii) the photocatalytic mechanism; and (iii) oxidization of MB by  $\cdot OH$ .

According to the Fenton-like catalytic mechanism, the interfacial Fe atoms ( $\equiv Fe^{III}$ ) can react with  $H_2O_2$  injected into the test solution to form  $\cdot OH$  as shown in Eq(3-5) (Li et al., 2017).



According to the photocatalytic mechanism, ReFeO<sub>3</sub> absorbs the visible light and undergoes charge separation and then generates  $\cdot OH$  as shown in Eq(6-8) (Thirumalairajan et al., 2013).



The conversion efficiency of MB by the NdFeO<sub>3</sub> catalyst was only 79.1 %, which is lower than that of ReFeO<sub>3</sub> after 3 h of illumination under visible light (Figure 4a). This is ascribed to the higher pore volume and pore size as well as the presence of some rare earth elements such as Pr, Dy and Tb in the composition of the ReFeO<sub>3</sub>.

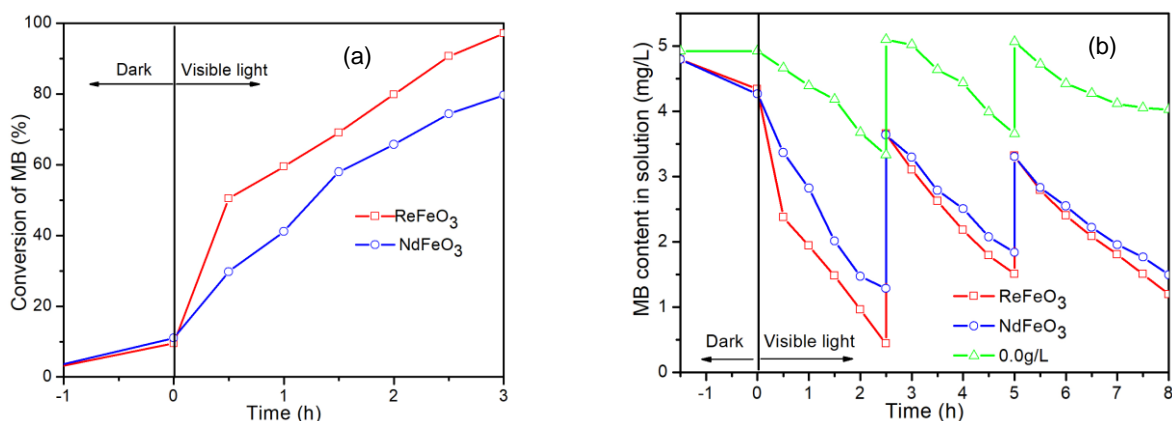


Figure 4: (a) Comparison of degradation efficiency between ReFeO<sub>3</sub> and NdFeO<sub>3</sub> (temperature = 35 °C; H<sub>2</sub>O<sub>2</sub> = 2 mL; m<sub>catalyst</sub> = 0.4 g/L) and (b) continuous test.

To clarify the superior photocatalytic property of ReFeO<sub>3</sub>, the degradation of MB was recorded under consecutive illumination of visible light. In specific, the first cycle was implemented at the same testing condition as the previous experiments. For each next cycle, 50 mL of MB was added to the test solution. As seen in Figure 4b, with the same subsequent illumination period of 2.5 h, the degradation efficiency of MB was quite good but still lower than that of the first cycle. This is due to the change in the ratio of catalyst weight and the solution volume as well as the decrease in the oxidizing agent H<sub>2</sub>O<sub>2</sub>. It means that the degradation of MB would increase continuously with the increase in the illuminate period. This obtained result implies the high success when ReFeO<sub>3</sub> is used as photocatalyst for wastewater treatment under continuous flow conditions.

For practical wastewater treatment applications, the stability and reusability of the catalysts play important roles. Thus, to evaluate photocatalytic capacity, the ReFeO<sub>3</sub> was recovered by centrifugation and then washed by distilled water at the end of each catalytical cycle. The received results are illustrated in Figure 5a. The degradation efficiency of MB slightly decreased from the first cycle to the fifth cycle, indicating high photocatalytic stability of ReFeO<sub>3</sub>. XRD pattern of ReFeO<sub>3</sub> was measured after 5 cycles of photodegradation for MB. It can be observed from Figure 5b that the reflection peaks located at the same positions. This demonstrates high stability in crystalline structure of ReFeO<sub>3</sub>.

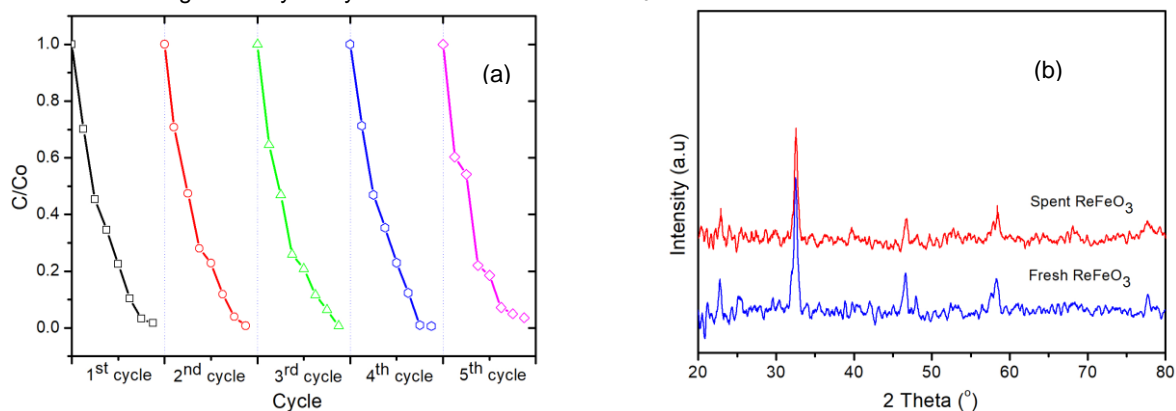


Figure 5: (a) Stability of ReFeO<sub>3</sub> over photodegradation of MB in five cycling runs and (b) XRD patterns of fresh and spent ReFeO<sub>3</sub> after 5 cycles of photodegradation of MB

#### 4. Conclusions

Perovskite ReFeO<sub>3</sub> has been successfully synthesized by the sol-gel citrate method from oxalate salt recovered from discarded magnets. Analysis results showed that the band-gap energies, pore volume and pore size parameters of the synthesized perovskite ReFeO<sub>3</sub> were higher than those of NdFeO<sub>3</sub> synthesized from pure salt. Synthesized ReFeO<sub>3</sub> material was used as a photocatalyst for the degradation of methylene blue under visible light. Experimental results showed that the degradation efficiency of MB could reach 99.2% and its photocatalytic capacity remained after 5 cycles. Photocatalytic activity of the perovskite material

synthesized from recovered rare earth was higher than that from the pure salt. Research results proved the high application potential of synthesized perovskite  $\text{ReFeO}_3$  material from e-waste source as a photocatalyst in treatment of organic pollutants like MB in wastewater sources.

### Acknowledgments

The authors acknowledge technical assistance from the School of Environmental Science and Technology and School of Chemical Engineering of Hanoi University of Science and Technology and Hanoi University of Mining and Geology.

### References

- Baldé C.P., Wang F., Kuehr R., Huisman J., 2015, The global e-waste monitor - 2014, United Nations University, IAS – SCYCLE, Bonn, Germany.
- Charalampides G., Vatalis K.I., Apostoplos B., Nikolas P.B., 2015, Rare earth elements: Industrial applications and economic dependency of Europe. *Procedia Economics and Finance*, 24, 126-135.
- Gao Z., Mogni L.V., Miller E. C., Railsback J. G., Barnett S. A., 2016, A perspective on low-temperature solid oxide, fuel cells, *Energy & Environmental Science*, 9, 1602-1644.
- Hao Y., Li B., Liu R., Li F., 2011, Synthesis of  $\text{NdFeO}_3$  perovskites in a reverse microemulsion and its visible light photocatalytic activity, *Advanced Materials Research*, 282-283, 593-596.
- Li L., Wang X., Lan Y., Gu W., Zhang S., 2013, Synthesis, photocatalytic and electrocatalytic activities of wormlike  $\text{GdFeO}_3$  nanoparticles by a glycol-assisted sol-gel process, *Industrial & Engineering Chemistry Research*, 52, 9130-9136.
- Luu M.D., Dao N.N., Nguyen V.D., Pham N.C., Vu T.N., Doan T.D., 2016, A new perovskite-type  $\text{NdFeO}_3$  adsorbent: synthesis, characterization, and As(V) adsorption, *Advances in Natural Sciences: Nanoscience and Nanotechnology*, 7, 025015.
- Nguyen D.Q., Yamasue E., Okumura H., Ishihara K.N., 2009, Use and disposal of large home electronic appliances in Vietnam. *Journal of Material Cycles Waste Management*, 11, 358-366.
- Phan T.T.N., Nikoloski A.N., Bahri P.A., Li D., 2017, Heterogeneous photo-fenton degradation of organics using highly efficient Cu-doped  $\text{LaFeO}_3$  under visible light, *Journal of Industrial and Engineering Chemistry*, 61, 53-64.
- Pham K. H., Nguyen T.T.H., Tran T.T.T., Huynh T.H., Mai T.T., 2017, Recovering rare earth oxide from  $\text{NdFeB}$  magnet of waste HDDs by leaching and selective precipitation methods, *Vietnam Journal of Science and Technology*, 55, 257-264.
- Sacco O., Vaiano V., Han C., Sannino D., Dionysiou D.D., Ciambelli P., 2015, Long Afterglow Green Phosphors Functionalized with Fe-N Doped  $\text{TiO}_2$  for the Photocatalytic Removal of Emerging Contaminants, *Chemical Engineering Transactions*, 43, 2107-2112.
- Tahir M., 2018, Photocatalytic carbon dioxide reduction to fuels in continuous flow monolith photoreactor using montmorillonite dispersed  $\text{Fe/TiO}_2$  nanocatalyst, *Journal of Cleaner Production*, 170, 242-250.
- Thirumalairajan S., Girija K., Hebalkar N.Y., Mangalaraj D., Viswanathan C., Ponpandian N., 2013, Shape evolution of perovskite  $\text{LaFeO}_3$  nanostructures: a systematic investigation of growth mechanism, properties and morphology dependent photocatalytic activities, *RSC Advances Journal*, 3, 7549-7561.
- Vaiano V., Iervolino G., Sannino D., 2017, Enhanced photocatalytic hydrogen production from glucose on Rh-doped  $\text{LaFeO}_3$ , *Chemical Engineering Transactions*, 60, 235-240.
- Willa C., Schmid A., Briand D., Yuan J., Koziej D., 2017, Lightweight, room-temperature  $\text{CO}_2$  gas sensor based on rare-earth metal-free composites - An impedance study, *ACS Applied Materials & Interfaces*, 9, 25553-25558.
- Yahya N., Aizat A., Sahrudin M.A.H., Aziz F., Jaafar J., Lau W.J., Yusof N., Salleh W.N.W., 2018, Adsorption and photocatalytic study of integrated photocatalyst adsorbent (IPCA) using  $\text{LaFeO}_3$ -GO nanocomposites for removal of synthetic dyes, *Chemical Engineering Transactions*, 63, 517-522.